Journal of The Electrochemical Society, **165** (14) G163-G170 (2018)
0013-4651/2018/165(14)/G163/8/$37.00 © The Electrochemical Society

Design and Synthesis of Efficient Electrogenerated Chemiluminescent Emitters Derived from Pyrene

Maria V. Cappellari,[1,2] María I. Mangione,[3,z] Rolando A. Spanevello,[3] Gabriela Marzari,[1,2] Gustavo M. Morales,[1,2] and Fernando Fungo[1,2,z]

[1]*Departamento de Química, Universidad Nacional de Río Cuarto, Río Cuarto, Argentina*
[2]*Instituto de Investigaciones en Tecnologías Energéticas y Materiales Avanzados, UNRC-CONICET, Argentina*
[3]*Instituto de Química Rosario, Facultad de Ciencias Bioquímicas y Farmacéuticas, Universidad Nacional de Rosario - CONICET., S2002RLK Rosario, Argentina*

The design and synthesis of novel dendrimeric structures derived from a pyrene core with substituted triphenylamine and carbazole periphery demonstrated how molecular engineering allowed the fine tuning of the electrogenerated chemiluminiscence (ECL) properties. These two compound (Py-CBZ and Py-TPA) in comparison with the parent structures (Py and Py-Core) showed better chemical stability and anti-aggregation capability. At the same time, the photophysical ($^{Abs}\lambda_{max}$, E_{00}, $^{FL}\lambda_{max}$, Φ_{FL}), photochemical (oxygen quenching), electrochemical (redox potentials) and optoelectronic (HOMO-LUMO gap and their energy position) properties were modulated, resulting in obtaining two highly ECL emitting molecular structures (Py-CBZ and Py-TPA). This study showed that functionalization of organic dyes with redox moieties (with the proper linker and position) improved the radical stability and also, modulated the optoelectronic properties with the concomitant enhancement of the ECL performance and their potential use in applications such as organic light-emitting devices.
 [DOI: 10.1149/2.0881814jes]

Manuscript submitted August 6, 2018; revised manuscript received October 12, 2018. Published November 6, 2018.

ECL is a light emission process[1–4] which has been used in the field of sensors,[5] development of analytical methods,[6,7] bioanalysis and bioimaging,[8] among others.[9,10] Recently, the use of the electrochemical processes to operate light-emitting devices with unusual functionality has gained significant interest; for example, light-emitting electrochemical cells (LECs) containing a small amount of electrolyte within the emissive active layer.[11] The liquid nature of this kind of ECL systems allows the ECL emitter encapsulation between flexible substrates electrodes, which is a simple way to fabricate deformable light-emitting devices. Also, through the right selection of the ECL dyes mixtures, it is possible to effectively tune the emissive color of these devices by controlling the potential applied to the electrodes.[2] Despite of the remarkable ECL possibilities for real applications, challenges still remain to be solve in the development of ECL materials. Two main issues to be approached are to increase the limited ECL fluorophores library and to improve the dyes stability toward the degradation originated by the ECL process. Regarding stability, it is known that small organic molecules used in optoelectronic applications undergo chemical degradation induced by water and oxygen.[12,13] This deleterious process can increase when the dyes excited states have long lifetime, which allows reaction to take place in the diffusional times of the species. Good candidates for ECL must be excellent emitting centers with good cation-anion radical chemical stability.[2] Among the organic ECL active materials, polycyclic aromatic hydrocarbons (PAH) and their derivatives are classical examples, for instance, 9,10-diphenylanthracene (DPA) and rubrene are used as ECL standards compounds.[2] Pyrene (Py) is an electrochemical active center with unique photophysical properties, presenting high quantum fluorescence yields with a large Stokes shift and its light emission is sensitive to micro-environmental changes, among others.[4,14–16] These properties make Py an excellent candidate to be used in ECL applications. However, Py has problems associate with its intrinsic properties that decrease its capability to produce efficiently ECL signal. Like many other organic centers with ECL potential, Py is a flat molecule that favors electrostatic interaction between molecular excited states, which decreases its quantum fluorescence yields. In addition, Py is a center that produces radical cation and anion with poor chemical stability.[17] The long lifetime of the Py excited states facilitates strong interaction with oxygen, hence quenching the light emitting process and producing singlet oxygen, a highly reactive species undesired in operating ECL devices.[12,18] Based on these factors, a Py center is not a good candidate for ECL.[16] This weaknesses can be overcome using Py core as dendrimeric framework of new molecular structures with improved optoelectric properties. Developments in Py core derivatives have been mushrooming in recent years.[19] Several synthetic modifications and functionalizations methodologies were reported in order to construct fluorescent probes and organic semiconductor materials.[19]

This work describes the synthesis, electrochemical reduction and oxidation and radical ion annihilation ECL of three Py derivatives, which were modified through the introduction of different electron donor-acceptor groups, conjugated bridges and bulky moieties (See Figure 1). The Py was utilized as a platform to introduce acetylene bonds to extend the intramolecular π-conjugation, block the reactive Py positions and bridged the conjugated core with triphenylamine (TPA) and carbazole (CBZ) electron donor groups. In addition, these electron donor groups were substituted with bulky moieties to produce steric hindrance effect in order to control the intermolecular interactions and to avoid the typical dimerization process that affects both aromatic-amine centers.[20–22] It has been reported that the use of a weakly donating group (*n*-propyl) or alkylamines as a substituent at the *para*-position of the phenyl group for a series of phenylethynylpyrene derivatives greatly improved ECL of Py core.[23–25] However, alkylamines substituents showed lack of chemical stability that induces film formation on the electrode surface, which limits the use of these moieties for ECL applications.[24] Therefore, it is expected that the functionalization with redox moieties (in appropriate position and with the proper linker) would improve the radical stability and also, modulate the optoelectronic properties of organic dyes with the consequent enhancement of the dye ECL performance. The structures of the Py-CBZ and Py-TPA molecules are shown in Figure 1 where Py-Core is included as a model compound for comparative analysis.

Materials and Methods

Instrumentation and characterization techniques.—The optical characterization was made using a diode array spectrometer Agilent 8453 and a spectrofluorometer Spex FluoroMax. Spectra were acquire using quartz cells (path length: 1 cm) at room temperature in *1,2*-dichloroethane (DCE) and toluene (PhMe) solutions. The emission spectra were measured between ~280–800 nm, exciting the maximum of the lower light absorption energy bands. For relative quantum fluorescence yields calculations 9,10-diphenylanthracene (DPA, Sigma-Aldrich) was used as an actinometer ($\Phi = 0.90$), which was dissolved in cyclohexane (Cicarelli, refractive index, $\eta = 1.427$), previously purified by simple distillation.

[z]E-mail: mangione@iquir-conicet.gov.ar; ffungo@exa.unrc.edu.ar

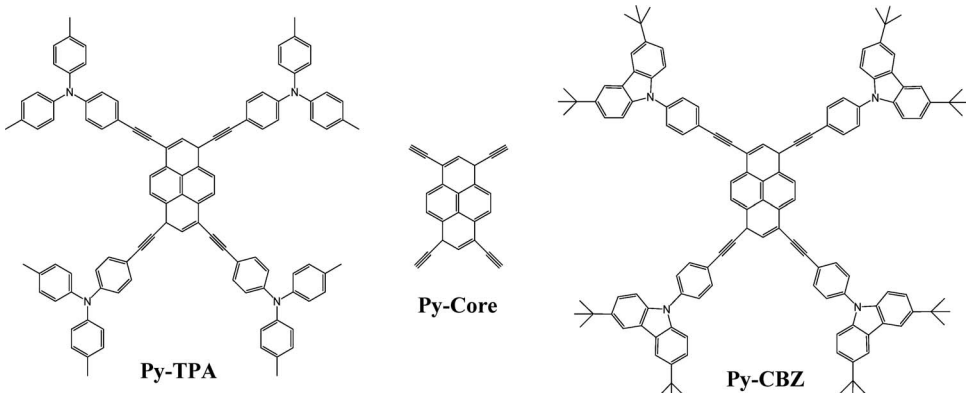

Figure 1. Pyrene derivatives molecular structures.

Electrochemical properties.—The electrochemical experiments were made in a potentiostat CH Instrument, model 700 E. The concentrations of the dyes under study were in the range of 0.5–1.0 mM in *1,2*-dichloroethane (DCE, Sintorgan), which was purified by simple distillation and stored over molecular sieves (Biopack, 3 Å) and $CaCO_3$ (Riedel-de Haën, 95%) containing 0.1 M of Tetrabutylammonium hexafluorophosphate (TBAHFP, purity >99%, Fluka) as the support electrolyte. The voltammetric experiments were carry out using as working electrode an inlaid platinum disk (0.0314 cm^2) polished on a felt pad with 0.3 μm alumina and sequentially sonicated in water and absolute ethanol. Before starting each electrochemical measurement, the Pt electrodes were tested by cyclic voltammograms in 1 M sulfuric acid (Cicarelli, 95–98%) in order to verify the correct cleaning of its surface. Silver wire was used as pseudo-reference electrode and a platinum coil as the counter electrode. Before each experiment electrolyte blank was made to discard possible electrochemically active interferences. All potential values reported are expressed relative to ferrocene/ferrocenium redox couple (Fc/Fc^+ = 0.40 V vs SCE), which was used as an internal standard.[26]

ECL characterization.—All the ECL measurements were made in a three electrode homemade electrochemical cell, which is adapted to a spectrofluorometer Spex Fluoromax. The cell holds a working electrode (Pt disc, diameter: 2mm) supported on glass, which has a 90° curvature that allows the Pt disc (electro-active region of the electrode) to be focused on the fluorometer detector. The Pt electrode was conditioned in the same way than the electrodes utilized for the electrochemical studies. The dyes ECL emission efficiencies (Φ_{ECL}) were determined by the number of photons emitted per injected electron relative to the known rubrene ECL efficiency under the same experimental conditions.[2,27,28] The electrochemical current and ECL were generated by applying three potential step waveform to the working electrode and the generated signals were registered in function on time. The three-step pulsed amperometric waveform was defined by the following parameters E1 = 0 V by 4 s, E2 = dye oxidation potential 0.2 s and E3 = dye reduction potential 0.2 s. This perturbation was applied three consecutive time and the obtained ECL and currents signals were integrated and used to estimate the dyes Φ_{ECL}. The ECL was recorded at the maximum wavelength corresponding to the ECL emission of each molecule and the fluorometer slit was opened 7 mm in order to collect as much light as possible. For the ECL measures, the co-reactants tripropylamine (nPr_3N, Sigma-Aldrich) and tetrabutylammonium persulfate ($(TBA)_2S_2O_8$) were used. $(TBA)_2S_2O_8$ was synthesized by a metathesis reaction between ammonium persulfate (Cicarelli) and tetrabutylammonium hydroxide (Sigma-Aldrich).[29]

Results and Discussion

Synthesis and characterization.—The synthetic pathway and the structures of the compound involved are depicted in Schemes 1 to 3. The Ullmann C-N and Sonogashira coupling reactions were the two main chemical transformations applied to construct the core, dendron and dendrimer structures. Starting with commercial Py (**1**), reaction with bromine as electrophile in nitrobenzene produced the tetrabromo derivative **2** in excellent yield.[30] This light green solid is insoluble in common organic solvents and its identity was verified by ESI, observing the pattern of masses corresponding to a compound with four bromine atoms. The coupling of **2** with commercial trimethylsilylacetylene under Pd-catalyzed conditions generated compound **3** as a bright orange solid. The trimethylsilyl protecting group was removed with anhydrous K_2CO_3 in methanol, yielding Py-Core, with excellent overall yield. The structures of **3** and Py-Core were confirmed by ^1H NMR spectroscopy and corroborated with the data published in the literature.[31] Py-Core was obtained as a yellowish solid and was the nucleus used for the preparation of the dendrimers (Scheme 1).

On the other hand and concomitantly with the construction of the pyrene nucleus, the synthesis of dendrons **7** and **11** were achieved. The preparation of 3,6-di-*tert*-butyl-9-(4-iodophenyl) **7** started with a Friedel-Crafst alkylation of commercial carbazole **4** with *tert*-butyl chloride to afford compound **5** in good yield.[32] Di-*tert*-butyl derivative **5** was treated under Ullmann modified conditions with 1,4-diiodocarbazole **6** to obtain compound **7** in 67% yield. Dendron **7** was characterized by ^1H and ^{13}C NMR and the data collected were according to those published in the literature[33] (Scheme 2).

The synthesis of the second dendron: *N,N-di*(4-tolyl)-4'-iodophenylamine **11** was also achieved in a straightforward manner. A ready available *di*-tolylamine **8** was coupled with iodobenzene **9** using a modified Ullmann protocol.[34] The substituted triphenylamine derivative **10** obtained in this way was subjected to an aromatic iodination procedure to afford **11** in good yield (Scheme 3).[35]

In a convergent synthetic strategy, Py-Core and the dendrons **7** and **11** were coupled applying Sonogashira reaction conditions to obtain dendrimers Py-CBZ and Py-TPA respectively in moderated yields (Scheme 4).[36] It is important to point out that it was necessary to place the terminal aryl alkyne on the core Py system and the aryl halide on the dendrons in order to avoid Glasser coupling[37] between dendrons and improve the yields of dendrimers. Dendrimer Py-CBZ is a bright orange solid while dendrimer Py-TPA is a bright red one. These compounds were fully charactherized by uni- and bi-dimensional ^1H and ^{13}C NMR spectroscopy, IR and MALDI-TOF spectrometry, all the data collected confirmed the expected structures.

Optical properties.—UV-visible light absorption and fluorescence emission spectra were used to analyze the photophysical properties of the molecules. The spectra showed in Figure 2 were obtained in DCE diluted solutions where dyes aggregation effect was not detected and therefore, the reported fluorescence data represent the monomer emission. Also, to facilitate a comparative analysis in this figure the typical Py absorption spectrum is included[18] and the main optical parameters obtained for the dyes are summarized in Table I. The

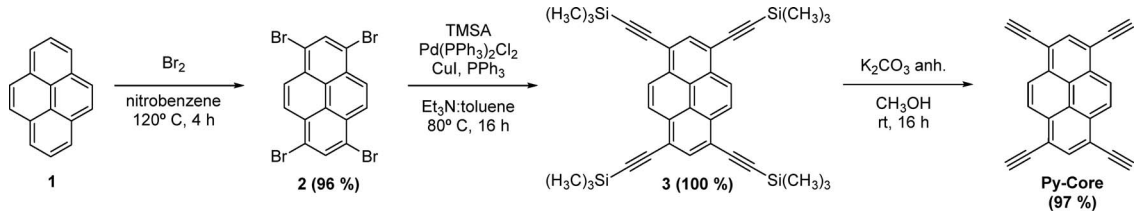

Scheme 1. Synthesis of Py-Core.

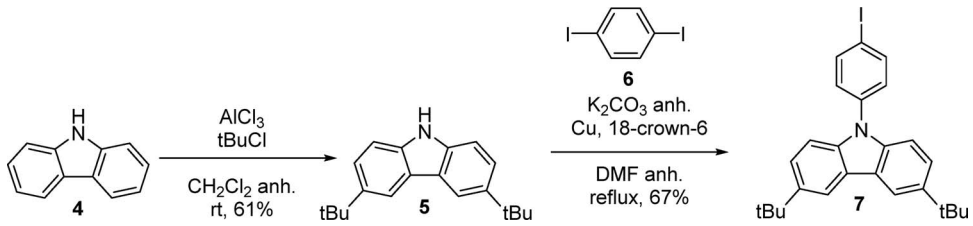

Scheme 2. Synthesis of dendron **7**.

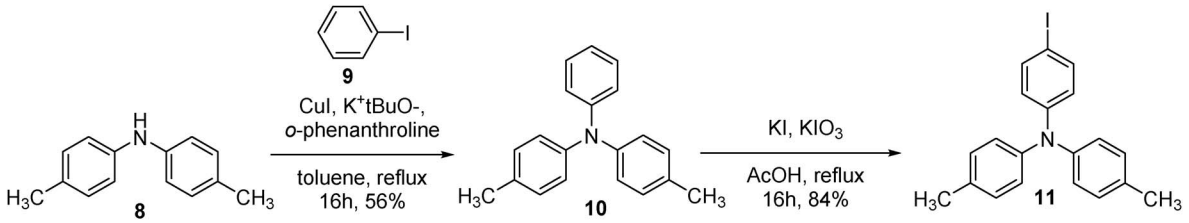

Scheme 3. Synthesis of dendron 11.

Table I. Photophysical and electrochemical properties.

	Py	Py-Core	Py-CBZ	Py-TPA
photophysic				
$^{Abs}\lambda_{máx}$ (nm)[a]	262, 270, 276, 306, 321, 337	295, 308, 373, 392, 419	287, 297, 337, 388, 458, 485	300, 344, 414, 482, 521
$^{FL}\lambda_{máx}$ (nm)[b]	370, 381, 392	420, 445	511	573
ε_{abs} (M^{-1} cm^{-1})[c]	21,625	14,085	68,316	44,987
Φ_{FL}[d]	0.008–0.261*	0.986	0.835	0.456
E_{00} (eV)[e]	3.57	2.96	2.53	2.28
Electrochemistry				
Epc (V)[f]	0.98	1.01	0.71–1	0.52–0.92
$Ec_{1/2}$ (V)[f]	-	-	0.68–0.96	0.47–0.88
Epa (V)[f]	−2.54	−1.79	−1.75	−1.85
$Ea_{1/2}$ (V)	−2.47	−1.77	−1.71	−1.82
ECL				
$-\Delta H_{an}$ (eV)[g]	3.42	2.70	2.36	2.27
HOMO (eV)[h]	−6.08	−6.11	−5.78	−5.57
LUMO (eV)[h]	−2.93	−3.15	−3.25	−3.29
$^{ECL}\lambda_{máx}$ (nm)[i]	472	-	531	606
Φ_{ECL}[j]	0.0008	-	0.24	0.41

*Fluorescence quantum yield in presence of oxygen and in degassed solution by bubbling Ar.
[a]Absorption spectra obtained in DCE.
[b]Emission spectra obtained in DCE.
[c]Calculated by Lambert-Beer law.
[d]Fluorescence quantum yield obtained in DCE. Standard used were 9,10-diphenylanthracene. Φ_{FL} (9,10-diphenylanthracene) = 1 in cyclohexane.[47]
[e]E_{00} calculated from UV/vis absorption and fluorescence spectra.
[f]All electrochemical data referenced versus ferrocene/ferrocenium couple.[26]
[g]Calculated from the difference between the two redox peak potentials.[2,26]
[h]HOMO calculated from voltammetric data as of HOMO = -($Ec_{1/2}$ + 5.1) eV. and LUMO = -(E_{00}-HOMO) eV.[2]
[i]ECL spectra obtained in DCE.
[j]ECL quantum yield obtained in DCE. Standard used were rubrene. Φ_{ECL} = 1 in DCE.[2]

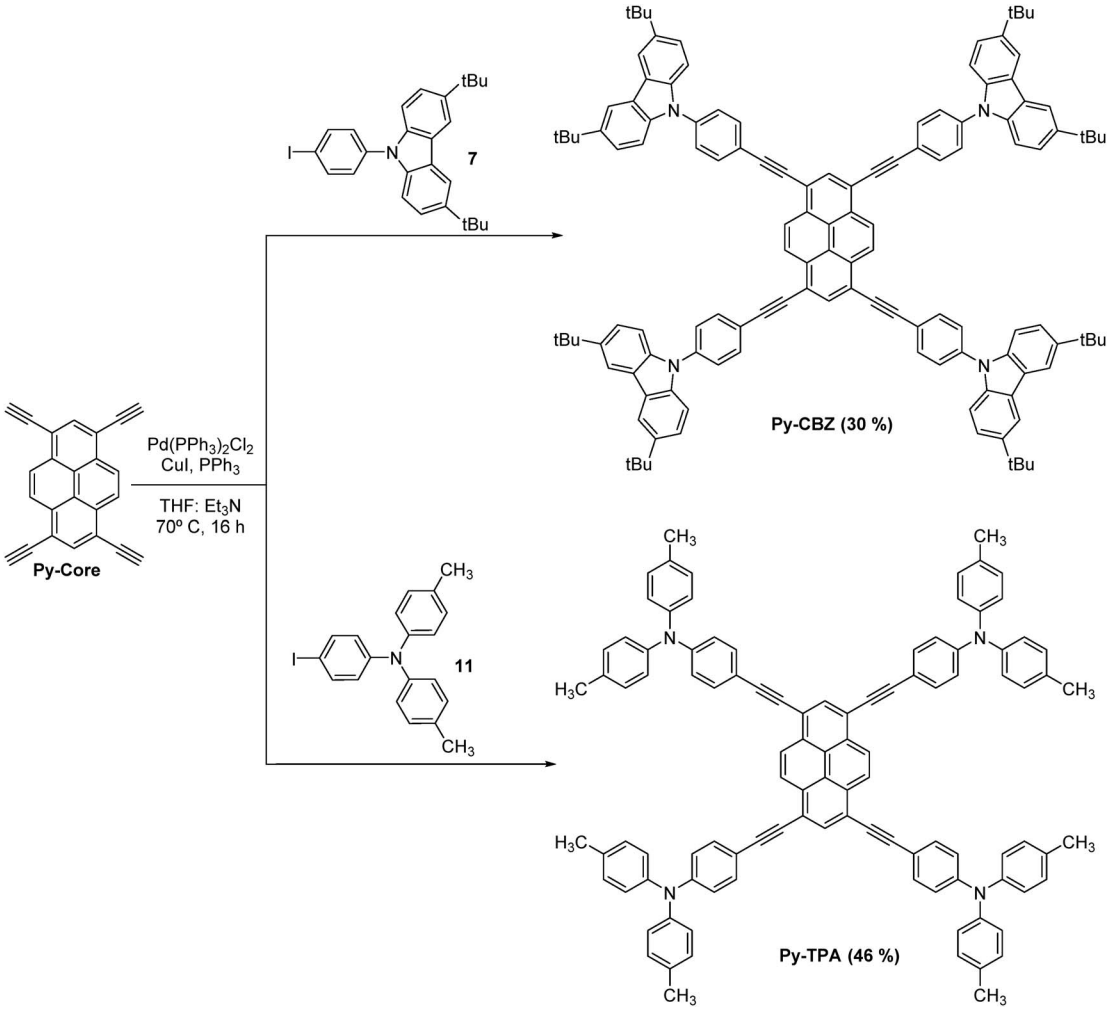

Scheme 4. Synthesis of dendrimers Py-CBZ and Py-TPA.

Py-Core presented absorption maxima at 308 nm, 373 nm, 392 nm and 419 nm, which are red shifted regarding Py (See Figure 2 and Table I). Photophysical properties of Py exhibit strong positional substitution dependence since these parameters are affected by the π-conjugated length of its molecular structure.[18,36,38] Thus, the observed bathochromic displacement in Py-Core was due to an increase in the molecular π-conjugation by the addition of the alkyne groups in positions 1-, 3-, 6- and −8.[30] On the other hand, Py-CBZ and Py-TPA have the electron donating CBZ and TPA moieties, respectively, linked by the acetylene bridge conjugated to the Py framework (See Figure 1). Consequently, it was expected that the strong electron-donating nature of these aromatic amines groups could affect the dye electron density and HOMO-LUMO distribution with a concomitant effect on the optical gap and the HOMO-LUMO energy position (see below the electrochemical characterization).[36,38,39] Py-CBZ showed absorption maxima in the same UV-energy region of the spectrum like Py and Py-Core (See Figure 2 and Table I). However, new absorption bands at 458 nm and 485 nm appeared, which could not be assigned to the introduction of the acetylene-CBZ residue (See spectrum of dye 1 in Ref. 40). Therefore, the spectrum was not a linear combination of the chromophores present in the dye molecular structure and this indicated a strong interaction between the constituent functional groups of the molecule. All the orbitals involved in the Py optical transitions have nonzero contributions at the 1-, 3-, 6-, and 8- positions, hence, significant influence in the Py-CBZ UV-spectra were expected.[18] In similar way, the introduction of a TPA substituent, which is a better electron donating group than CBZ,[40] produces light absorption red shifted regarding the observed in the Py-CBZ (see Figure 2 and Table I). All studied compounds showed no solvent dependence in their light absorption maxima values, which indicates a small dipole moment in their ground state.[41]

The fluorescence spectra of the dyes were studied in DCE and PhMe diluted solutions where the formation of aggregates was minimized and the results obtained are shown with a colored solid line in Figure 2 and summarized in Table I. Py-Core in PhMe solution showed maximum emission ($^{FL}\lambda_{max}$) at 420 nm and 445 nm and a shoulder at 477 nm. These maxima were red shifted regarding the Py as consequence of the increase in the molecular conjugation length due to the alkyne groups linked at 1-, 3-, 6- and 8- positions. Similar to Py, the Py-Core light absorption and emission behaviors held fine structures and they were quite insensitive to changes of solution polarity, indicating that there were not important differences between ground and excited states dipole moments. These photophysical characteristics were in good agreement with those ones reported for related molecular structures.[18,31,42] For Py-CBZ and Py-TPA their emission maxima were found at 506 nm and 538 nm in nonpolar PhMe solutions, respectively. As it was pointed out in the light absorption behavior analysis, it was expected that Py-TPA emited at a low energy than Py-CBZ. However, Py-TPA showed fluorescence maximum more sensitive to the solvent polarity changes than Py-CBZ. Figure 2 showed that the emission maxima of Py-TPA presented a bathochromic shift of ∼35 nm, while Py-CBZ only moved its maximum ∼5 nm, which would indicate that there was a moderate change of the dipole moment between the ground and excited state. The charge transfer strength variation between

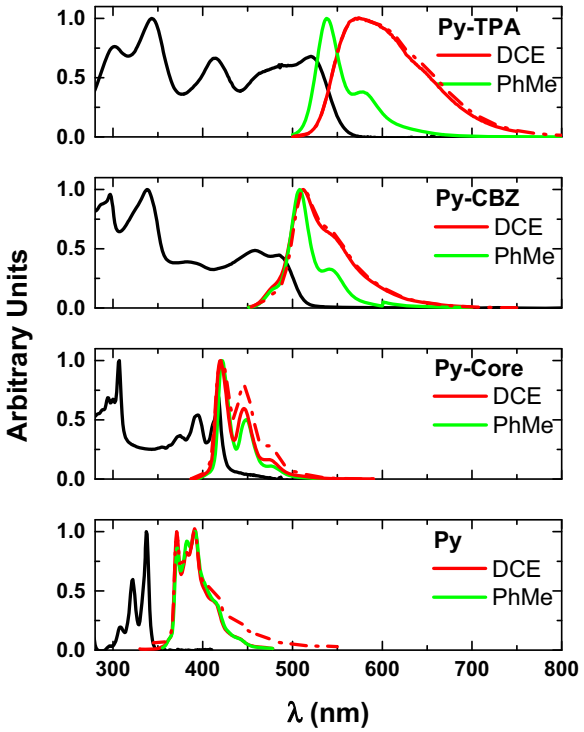

Figure 2. Normalized light absorption spectra (black solid line) obtained in DCE solution (5.10^{-7} M). Emission spectra obtained in DCE solution (5.10^{-7} M and 1.10^{-4} M, red solid and red dashed line, respectively) and PhMe solution (5.10^{-7} M, green solid line).

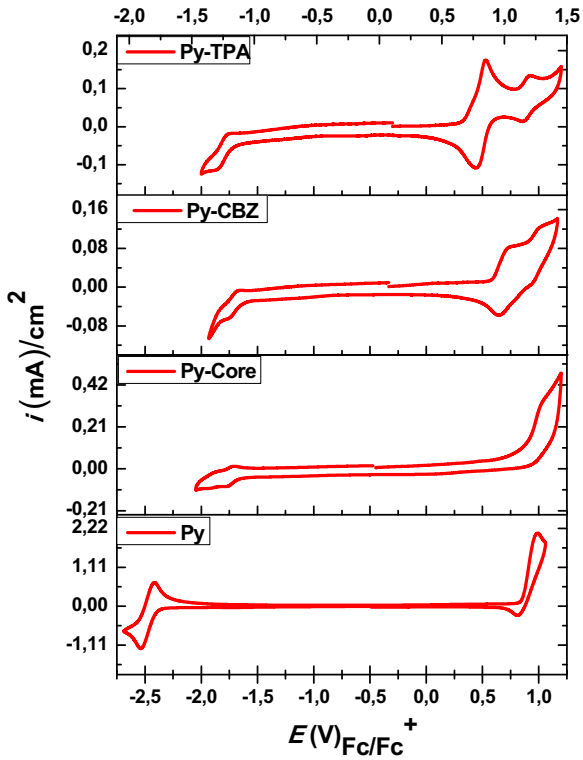

Figure 3. Cyclic voltammograms of the Py (∼1 mM) and Py-Core (∼0.5 mM) in 3:1 toluene/acetonitrile mixture and for Py-CBZ and Py-TPA (∼0.5 mM) in TBAHFP/3:1 toluene-acetonitrile mixture electrolyte. Pt electrode and scan rate = 100 mV s^{-1}.

Py-CBZ and Py-TPA was due to the smallest conjugation length present in Py-CBZ, which it was affected by the nonplanar orientations of the carbazolyl moieties[38,39,43] (See Figure 1). Also, TPA substituent is a better electron donor than CBZ centers,[40] which increases the intramolecular charge transfer character. Thus, the solvatochromism phenomenon effect in Py-TPA was more pronounced. It is interesting to note that commonly, the modulation of this solvatochromic property in Py derivatives is achieved by non-symmetrical substitution pattern and in the dyes under study, this effect was accomplished with symmetrical structures.[24,44]

The fluorescence quantum yields (Φ_{FL}) for each molecule were determined at room temperature in degassed and aerated DCE solutions and the observed values relative to the DPA are also listed in Table I. All the synthesized compounds have higher quantum yields values than the precursor Py. The rigid structure of Py allows efficient intersystem crossing pathway, and also produces singlet state with lifetime long enough to permit fluorescence quenching by oxygen diffusion, which decreases its emission efficiency.[13] Therefore, the high Φ_{FL} of the fluorophores shown in Figure 1 suggests that these light emission deleterious processes are inefficient. In agreement with these assumptions, when Φ_{FL} of the dyes were measured in presence of atmospheric oxygen, the fluorescence intensities of compounds Py-Core, Py-TPA and Py-CBZ were unaffected obtaining the same yields values before and after degassing; while Py Φ_{FL} was dramatically affected (See Table I). Notably, this oxygen insensibility is a highly desired property in optoelectronic application, because produces chemical stability in the excited states of the materials. On the other hand, Φ_{FL} values decrease in the following order Py-Core**,** Py-CBZ and Py-TPA in good concordance with the structural molecular characteristic. Py-Core was the most rigid structure, while the introduction of the aromatic amines in Py-CBZ and Py-TPA favors the free rotation of the phenyl substituents (specially for Py-TPA) in conjugation with the central pyrene, which allows competing non-radiative pathways for the decay of the excited singlet state.[42]

The dyes aggregated formation tendency was checked by taking the fluorescence spectra at different molar concentrations. In Figure 2 the emission spectra in DCE solution at 5.10^{-7} M (red solid line) and 10^{-4} M (red dashed line) are shown. As it was expected for the concentrated solution of Py, the typical light emission band related to the excimer formation appeared around at 450 nm.[12] A similar behavior was observed with Py-Core since the steric effect of the acetylenic substituents were not able to prevent the face-to-face π molecular interaction in solution. However, for Py-CBZ and Py-TPA the fluorescent spectra were not affected by concentration changes and the observed emission corresponded only to the monomers. Therefore, in these dyes the CBZ and TPA groups could avoid that two molecules get close enough to produce excimer emission, and similar results were observed even at high concentrations above 10^{-4} M. Thus, the fluorophores structural characteristics provided good explanations for the photophysical behaviors observed.

Electrochemical properties.—To perform the electrochemical measurements, TBAHFP/3:1 toluene-acetonitrile mixture electrolyte was used due to the low solubility that have Py and Py-Core. Figure 3 describes the cyclic voltammograms (CV) corresponding to the molecules showed in Figure 1, where differentiated redox behaviors were observed for each system. In a comparative analysis with related structures, the Py CV showed a reversible reduction process at ∼−2.54 V and an oxidation wave with maximum at ∼+0.98 V, which corresponds to the cation radicals formation with chemical instability in the CV time scale.[17] In the case of the remaining dyes, it was clear that both anodic and cathodic redox processes were affected, which indicates that functionalization effectively modified the Py electrochemical properties. It was notorious the shift on the reduction potentials, more than 0.75 V (See Table I), observed between the three modified dyes and Py itself. However, the differences of reduction potential values between Py-Core, Py-CBZ and Py-TPA

dyes were only ~0.1 V (See Table I). Therefore, these results suggested that the acetylene moieties were the main factor responsible for the observed reduction potential shift, while the nitrogen atoms of Py-CBZ and Py-TPA have a minor effect on the dyes reduction processes. The increment of the conjugation length has a greater influence on the orbitals energy level that participates in the reduction process than the electronegative effect that can exercise the nitrogen atom. On the other hand, in the analysis of the dyes' electrochemical behavior at positive potential (Figure 3), Py-Core showed an oxidation peak around +1.0 V with a wave shape characteristic of an irreversible electrochemical process. Comparing it with Py, revealed that the acetylene substituents do not affect the peak oxidation potential and also do not improve the stability of the formed radical cations. This lack of chemical stability can due to the presence of the labile hydrogen on terminal alkynes that facilitates the deprotonation of the electrochemically formed Py-Core radical cation.

Alternatively, the introduction of the aromatic amines in Py-TPA and Py-CBZ, changed radically the oxidation behavior of these dyes regarding Py and Py-Core. In the case of Py-CBZ, the detection of an oxidation wave with a shoulder at +0.71 V and +1.00 V, respectively, was observed in the current trace corresponding to the positive potential scan showed in Figure 3. When the potential sweep direction was inverted, both oxidation processes showed their complementary reduction waves at +0.64 V and +0.95 V, respectively, which indicated a good chemical stability of the generated charged species. CBZ had lower oxidation potential than Py,[20–22] therefore, the first electrochemically removed electron from Py-CBZ could be assigned to the CBZ moiety oxidation; while the second one corresponds to the Py ring. The good chemical stability observed for the Py-CBZ radical cation and dication compared with Py and Py-Core can be explained by two factors: a.- the effective increment in the conjugation extension achieved by bonding good electron donating groups (CBZ) to the Py ring via a triple bond in the 1-,3-,6-,8- reactive positions (See Figure 1); b.- the introduction of *tert*-butyl moieties in CBZ skeleton that stabilize its radical cation avoiding the dimerization process.[21,22] The analysis of the Py-TPA electrochemical behavior was similar to the one made with Py-CBZ. Likewise, Py-TPA showed two oxidation voltammetric waves with potential peaks at +0.52 V and +0.92 V (Figure 3). But in this case, the potential peaks maxima were shifted to lower potential and the waves are less overlapping than those observed for Py-CBZ. The TPA moiety is a better electron donor and it is easier to oxidize than CBZ group.[22] Therefore, the two oxidation waves were expected to move at lower potentials with respect to Py-CBZ. Nevertheless, this shift was more marked in the first wave than in the second one, which produced a definite separation of the voltammetric waves. Similarly to Py-CBZ, the TPA reactive positions were blocked with alkyl substituents, which stabilized its radical cation, avoiding the formation of tetraphenylbenzidine through a coupling-dimerization reaction.[21,22] Summarizing the electrochemistry of all the compounds, it could be observed a stability improvement of radical cation and anion species derived from Py-CBZ and the Py-TPA, which proved the success of the molecular design strategy to enhance the performance of the generated charged species. In this sense, Py-CBZ and the Py-TPA, which hold tertiary aromatic amines in their structure (See Figure 1), showed better radical cation behavior than *tetrakis*(ethynyl)pyrenes functionalized with *N,N*′-dialkylanilines. The last one showed instabilities in their charged species, which tends to form thin film on the electrode surface during the voltammetric cycling.[24] The HOMO and LUMO energy levels were calculated and the results are listed in Table I together with other electro-optical parameters. In agreement with the energy-gap (E_{00}) trends obtained from the spectroscopic studies, it was observed that the electrochemical gap (HOMO−LUMO) gradually decreased as the π-conjugation length and electron donor capability of the substituents increased. In another way, the position of the LUMO-HOMO in the absolute energy scale was shifted consequently with the electrochemical characteristic of the moieties bonded to the Py ring. For example, the dyes HOMOs were in the energy range expected for commonly phenylamine derived hole transporter layer materials used in optoelectronic applications.[22,45]

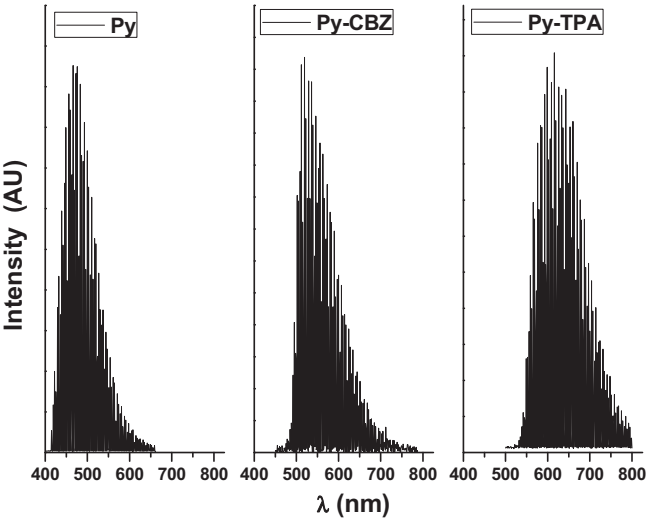

Figure 4. ECL spectra of pyrene derivatives system (~0.5 mM) in TBAHFP/DCE electrolyte with pulsing (10 Hz) between dyes reduction and oxidation peak potentials.

Finally, it was calculated the enthalpy energy ($-\Delta H_{an}$) available in the radical cation/radical anion annihilation reaction from the obtained dyes redox parameters.[1,3] This is an important ECL parameter that allows to evaluate whether the studied systems release enough energy to produce the emitting excited state through electrochemically induced reactions. Comparing the $-\Delta H_{an}$ values showed in Table I with the corresponding E_{00}, it could be noted that Py and Py-TPA are able to exergonically produce ECL ($-\Delta H_{an} > E_{00}$).[1,3] Considering that only Py-TPA combines a high quantum fluorescence yield, good charged species stability and sufficient ion annihilation enthalpy energy to populate directly their emitting excited states, it can be stated that this molecule is a promising candidate to efficiently produce ECL phenomenon.

Electrogenerated chemiluminescence properties.—In Figure 4 are shown the Py, Py-CBZ and Py-TPA ECL spectra registered under the same conditions used for electrochemical experiments (dyes concentration, electrolyte composition). The electrochemical cell was perturbed by a 10 Hz potential square-wave, which it was modulated by jumps between the oxidation and reduction potentials values, where radical cation and anion forms are alternately produced. These applied potentials were already determined and presented in the electrochemical section (Table I). The maximum of Py ECL signal ($^{ECL}\lambda_{max}$) was redshifted ~80 nm regarding its fluorescence maxima spectrum showed in Figure 1 and this behavior was ruled by the excimer formation, which emitted light at 470 nm.[46] While for the Py-Core, it was not possible to detect the ECL phenomenon in the used experimental conditions, even after the addition of anodic or cathodic co-reactants. This result was mainly due to the poor chemical stability of Py-Core charged species, which avoided in the experimental time scale their encounter, annihilation and formation of the excited light-emitting state processes. On the other hand, Py-CBZ and Py-TPA showed ECL activity with emission maxima at 531 nm and 606 nm, respectively. Previously, it was estimated that Py-CBZ had insufficient energy to populate their main emitting excited states ($-\Delta H_{an} < E_{00}$, See Table I). However, the fact that this dye was able to generate ECL signal, without use of co-reactants, it was an indicative that Py-CBZ could be classified as an energy-deficient system, where $-\Delta H_{an}$ is smaller than the first excited singlet state, but larger than its triplet state energy.[2]

Py-TPA was an active ECL substrate with enough energy to produce emitting states through electrochemical stimulation ($-\Delta H_{an} > E_{00}$, See Table I). Consequently, in Figure 4 it is shown a Py-TPA ECL spectrum with a broad band with maximum at 606 nm. In Table I could be observed that the Py-CBZ and Py-TPA ECL

$$\text{Py-D} - e^- \longrightarrow \text{Py}^{\bullet-}\text{-D} \quad (1)$$

$$\text{Py-D} + e^- \longrightarrow \text{Py-D}^{\bullet+} \quad (2)$$

$$\text{Py-D}^{\bullet+} + \text{Py}^{\bullet-}\text{-D} \longrightarrow {}^1(\text{Py}^{\bullet-}\text{-D}^{\bullet+})^* \quad (3)$$

$$\text{Py-D}^{\bullet+} + \text{Py}^{\bullet-}\text{-D} \longrightarrow {}^3(\text{Py-D})^* \quad (4)$$

$${}^3(\text{Py-D})^* + {}^3(\text{Py-D})^* \longrightarrow {}^1(\text{Py}^{\bullet-}\text{-D}^{\bullet+})^* + (\text{Py-D}) \quad (5)$$

$$(\text{Py}^{\bullet-}\text{-D}^{\bullet+})^* \longrightarrow \text{Py-D} + \text{luz} \quad (6)$$

Scheme 5. ECL emission mechanism of Py derivatives, where D is CBZ or TPA. (1) and (2) radical cation and anion electrochemical formation. (3) and (4) radical cation/radical anion annihilation reactions. (5) Triplet-triplet annihilation reaction. (6) ECL emission.

maxima were shifted about 20 nm and 33 nm to lower energies regarding its fluorescence emission, respectively. This shifting could be attributed to self-absorption that allows the Stokes shift of these systems (See Figure 2). This filter effect was magnified due to the high concentration (mM range) used in the ECL experiments. Therefore, there is a good correlation between dyes ECL spectra and the corresponding fluorescence spectra. Py-TPA also showed a broadness spectrum, which can be associated to the previously observed intramolecular charge transfer character of the excite state of this molecule. Moreover, the low aggregation effect observed for Py-CBZ and Py-TPA in the photophysical study was retained in the ECL experiments due to their ECL spectra are insensitive to the dyes concentration changes, which it is a property wanted from an optoelectronic applications point of view. The mechanism showed in the Scheme 5 is consistent with the described ECL behavior for Py-CBZ and Py-TPA.

On the other hand, dyes ECL efficiencies were determined by the number of photons emitted per injected electron relative to the known rubrene ECL emission[2] and the calculated values are listed in Table I. A clear difference of several order of magnitude was observed between the ECL relative yields of Py and the ones measured for Py-CBZ and Py-TPA. Moreover, it is interesting to compare the relative ECL quantum yield: the reached value by Py-TPA was approximately twice as higher as the one found for Py-CBZ under the same experimental conditions, although Py-TPA photophysically emits half of light than Py-CBZ (See Φ_{ECL} and Φ_{FL} in Table I). This observed behavior could be related with the differences between the electron donating capability of TPA and CBZ moieties. As it was mentioned before, Py-CBZ was deficient in energy to directly produce ECL, while Py-TPA was not (See Scheme 5). It is expected that the TPA moieties bonded to the Py ring shift both, the oxidation potential and the emission maximum toward lower energy values regarding the CBZ; while the dyes reduction potential moves to more negative values. All these changes can be corroborated in Table I, however, these displacements were not affected in the same magnitude. Thus, the Py-TPA formal potential difference ($Ec_{1/2}$-$Ea_{1/2}$) was larger enough to provide the required driving force in the annihilation reaction for the efficient formation of ECL emissive excited states. It was also observed for Py-TPA (Figure 3) that its radical cation formation occur reversibly at a well-defined potential, while the Py-CBZ first oxidation overlapped with the dication formation processes. Thus, Py-TPA has remarkable optoelectronic characteristics, which makes it the best ECL emitter within the studied dyes.

Conclusions

Polycyclic aromatic hydrocarbons are promising candidates for ECL applications due to the combination of an electrochemical active center with a high quantum fluorescence yields. However, some disadvantages such as the flat molecular structure, which favored light quenching through intermolecular interactions or formation of charged species with poor chemical stabilities, among others, decrease the efficiency to generate the ECL phenomenon. Notwithstanding, using molecular engineering all these drawbacks were systematically overcome by bonding electron donor moieties (CBZ or TPA) through unsaturated bridges (aryl alkyne) to Py reactive sites (1-, 3-, 6- and 8-positions). In addition, the blockade of reactive positions of CBZ and TPA with bulky alkyl groups avoids the typical coupling-dimerization reaction, stabilizing the radical cations on the dendritic structures. Simultaneously, the photophysical ($^{Abs}\lambda_{max}$, E_{00}, $^{FL}\lambda_{max}$, $\Phi_{FL}{}^d$), photochemical (low aggregation effect and oxygen quenching), electrochemical (redox potentials) and optoelectronic (HOMO-LUMO gap and their energy position) properties were tuned in order to obtain two molecules with a high ECL emitting yield (Py-CBZ and Py-TPA). Hence, the used molecular design strategy succeed in produce new dyes which efficiently emit ECL light. This study demonstrate that the functionalization of organic dyes with redox moieties (in the adequate positions and with the proper linker) allows to improve the radical stability and modulate the optoelectronic properties with the consequent enhancement of the ECL performance and their potential use in applications such as organic light-emitting devices.

Acknowledgments

We thank Consejo Nacional de Investigaciones Científicas y Técnicas (CONICET-Argentina), Agencia Nacional de Promoción Científica y Tecnológica (ANPCYT Argentina), Universidad Nacional de Rosario y Universidad Nacional de Río Cuarto. M.I.M, R.A.S, M.V.C, G.M.M, and F.F. are scientific members of CONICET.

ORCID

María I. Mangione https://orcid.org/0000-0003-4264-4392
Rolando A. Spanevello https://orcid.org/0000-0003-3701-5807
Fernando Fungo https://orcid.org/0000-0003-3291-0829

References

1. A. J. Bard and L. R. Faulkner, *Electrochemical Methods: Fundamentals and Applications*, 2nd Edition, John Wiley & Sons, Inc., New York (2001).
2. A. J. Bard, *Electrogenerated Chemiluminescence*, Marcel Dekker, New York (2004).
3. L. R. Faulkner and A. J. Bard, in *Electroanal. Chem.*, A. J. Bard, ed., p. 1, Dekker, New York, (1977).
4. M. Hesari and Z. Ding, *J. Electrochem. Soc.*, **163**, H3116 (2016).
5. J. Sun, H. Sun, and Z. Liang, *ChemElectroChem*, **4**, 1651 (2017).
6. G. Marzari, M. V. Cappellari, G. M. Morales, and F. Fungo, *Anal. Methods*, **9**, 2452 (2017).
7. J. Sun, W. Gao, L. Qi, Y. Song, P. Hui, Z. Liu, and G. Xu, *Anal. and Bioanal. Chem*, **410**, 2315 (2018).
8. J. L. Liu, M. Zhao, Y. Zhuo, Y. Q. Chai, and R. Yuan, *Chem. Eur. J.*, **23**, 1853 (2017).
9. K. Hong, M. G. Kim, H. M. Yang, D. C. Lim, J. Y. Lee, S. J. Kim, I. Lee, K. H. Lee, and J. L. Lee, *Adv. Energy Mater.*, **6** (2016).
10. T. Kasahara, S. Matsunami, T. Edura, R. Ishimatsu, J. Oshima, M. Tsuwaki, T. Imato, S. Shoji, C. Adachi, and J. Mizuno, *Sens. Actuators, B*, **207**, 481 (2015).
11. S. H. Kong, J. I. Lee, S. Kim, and M. S. Kang, *ACS Photonics*, (2017).
12. N. J. Turro, V. Ramamurthy, and J. C. Scaiano, *Principles of molecular photochemistry: an introduction*, University science books (2009).
13. M. Hermenau, M. Riede, K. Leo, S. A. Gevorgyan, F. C. Krebs, and K. Norrman, *Sol. Energy Mater. Sol. Cells*, **95**, 1268 (2011).

14. T. M. Figueira-Duarte and K. Müllen, *Chem. Rev.*, **111**, 7260 (2011).
15. K. Kalyanasundaram and J. Thomas, *J. Am. Chem. Soc.*, **99** (1977).
16. J. Maloy and A. J. Bard, *J. Am. Chem. Soc.*, **93**, 5968 (1971).
17. M. M. Richter, *Chem. Rev.*, **104**, 3003 (2004).
18. A. G. Crawford, A. D. Dwyer, Z. Liu, A. Steffen, A. Beeby, L.-O. Paålsson, D. J. Tozer, and T. B. Marder, *J. Am. Chem. Soc.*, **133**, 13349 (2011).
19. X. Feng, J. Y. Hu, C. Redshaw, and T. Yamato, *Chem. Eur. J.*, **22**, 11898 (2016).
20. F. Fungo, K.-T. Wong, S.-Y. Ku, Y.-Y. Hung, and A. J. Bard, *J. Phys. Chem. B*, **109**, 3984 (2005).
21. J. Natera, L. Otero, L. Sereno, F. Fungo, N.-S. Wang, Y.-M. Tsai, T.-Y. Hwu, and K.-T. Wong, *Macromolecules*, **40**, 4456 (2007).
22. D. Heredia, J. Natera, M. Gervaldo, L. Otero, F. Fungo, C.-Y. Lin, and K.-T. Wong, *Org. Lett.*, **12**, 12 (2009).
23. Y. O. Lee, T. Pradhan, K. Choi, D. H. Choi, J. H. Lee, and J. S. Kim, *Tetrahedron*, **69**, 5908 (2013).
24. Y. O. Lee, T. Pradhan, S. Yoo, T. H. Kim, J. Kim, and J. S. Kim, *J. Org. Chem.*, **77**, 11007 (2012).
25. J. W. Oh, Y. O. Lee, T. H. Kim, K. C. Ko, J. Y. Lee, H. Kim, and J. S. Kim, *Angew. Chem. Inter. Ed.*, **48**, 2522 (2009).
26. C. M. Cardona, W. Li, A. E. Kaifer, D. Stockdale, and G. C. Bazan, *Adv. Mater.*, **23**, 2367 (2011).
27. K. M. Omer, S. Y. Ku, K. T. Wong, and A. J. Bard, *Angew. Chem. Inter. Ed.*, **48**, 9300 (2009).
28. M. Hesari, K. N. Swanick, J.-S. Lu, R. Whyte, S. Wang, and Z. Ding, *J. Am. Chem. Soc*, **137**, 11266 (2015).
29. I.-S. Shin, S. Yoon, J. I. Kim, J.-K. Lee, T. H. Kim, and H. Kim, *Electrochim. Acta*, **56**, 6219 (2011).
30. G. Venkataramana and S. Sankararaman, *Eur. J. Org. Chem.*, **2005**, 4162 (2005).
31. Z.-Q. Liang, Z.-Z. Chu, J.-X. Yang, C.-X. Yuan, X.-T. Tao, and D.-C. Zou, *Synthetic Metals*, **161**, 1691 (2011).
32. M. I. Mangione and R. A. Spanevello, *Tetrahedron Lett.*, **56**, 465 (2015).
33. Y. Xing, X. Xu, P. Zhang, W. Tian, G. Yu, P. Lu, Y. Liu, and D. Zhu, *Chem. Phys. Lett.*, **408**, 169 (2005).
34. C. K. Tseng, C. R. Lee, M. C. Tseng, C. C. Han, and S. G. Shyu, *Dalton Trans.*, **43**, 7020 (2014).
35. J. Chen, S. Ko, L. Liu, Y. Sheng, H. Han, and X. Li, *New J. Chem.*, **39**, 3736 (2015).
36. J. y. Hu, M. Era, M. R. Elsegood, and T. Yamato, *Eur. J. Org. Chem.*, **2010**, 72 (2010).
37. C. Glaser, *Ber. Dtsch. Chem. Ges.*, **2**, 422 (1869).
38. C.-Z. Wang, X. Feng, Z. Kowser, C. Wu, T. Akther, M. R. Elsegood, C. Redshaw, and T. Yamato, *Dyes Pigm.*, (2018).
39. S. N. Keller, A. D. Bromby, and T. C. Sutherland, *Eur. J. Org. Chem.*, **2017**, 3980 (2017).
40. M. I. Mangione, R. A. Spanevello, D. Minudri, D. Heredia, L. Fernandez, L. Otero, and F. Fungo, *Electrochim. Acta*, **207**, 143 (2016).
41. J. Sung, P. Kim, Y. O. Lee, J. S. Kim, and D. Kim, *J. Phys. Chem. Lett.*, **2**, 818 (2011).
42. H. Maeda, T. Maeda, K. Mizuno, K. Fujimoto, H. Shimizu, and M. Inouye, *Chem. Eur. J.*, **12**, 824 (2006).
43. K. C. Moss, K. N. Bourdakos, V. Bhalla, K. T. Kamtekar, M. R. Bryce, M. A. Fox, H. L. Vaughan, F. B. Dias, and A. P. Monkman, *J. Org. Chem.*, **75**, 6771 (2010).
44. Y. O. Lee, T. Pradhan, K. No, and J. S. Kim, *Tetrahedron*, **68**, 1704 (2012).
45. Y. Shirota and H. Kageyama, *Chem. Rev.*, **107**, 953 (2007).
46. B. Fleet, G. Kirkbright, and C. Pickford, *J. Electroanal. Chem. Interfacial Electrochem.*, **30**, 115 (1971).
47. I. Berlman, *Handbook of Fluorescence Spectra of Aromatic Molecules*, Academic Press, New York and London (1971).